Chemical Engineering Journal 306 (2016) 1017–1025

Contents lists available at ScienceDirect

Chemical Engineering Journal

journal homepage: www.elsevier.com/locate/cej

High-performance gas-liquid-solid microreactor with polydopamine functionalized surface coated by Pd nanocatalyst for nitrobenzene hydrogenation

Hao Feng, Xun Zhu *, Rong Chen, Qiang Liao, Jian Liu, Lin Li

Key Laboratory of Low-grade Energy Utilization Technologies and Systems (Chongqing University), Ministry of Education, Chongqing 400030, China
Institute of Engineering Thermophysics, Chongqing University, Chongqing 400030, China

HIGHLIGHTS

- A high-performance gas-liquid-solid microreactor was developed by electroless deposition.
- Polydopamine was used to functionalize the surface for coating nanocatalysts.
- The developed microreactor yielded high and stable performance.
- Parametric study was performed to optimize the microreactor operation.

ARTICLE INFO

Article history:
Received 12 February 2016
Received in revised form 3 July 2016
Accepted 3 August 2016
Available online 3 August 2016

Keywords:
Gas-liquid-solid microreactor
Polydopamine functionalized surface
Pd nanoparticle
Aniline concentration
Nitrobenzene conversion
Excess ratio

ABSTRACT

In this study, a gas-liquid-solid microreactor with the polydopamine functionalized surface coated by highly-active palladium nanocatalysts using the electroless deposition was successfully developed for hydrogenation of nitrobenzene. Experimental results showed that in the 40-h continuous operation, the developed microreactor exhibited rather high average nitrobenzene conversion more than 97% under various inlet nitrobenzene concentrations from 30 to 90 mM. Besides, the effect of the gas and liquid flow rates on the aniline concentration and nitrobenzene conversion was also studied. It was found that for a given liquid flow rate, the increase of the gas flow rate led to an increase in both the aniline concentration and nitrobenzene conversion as a result of more hydrogen supplied. Further increasing the gas flow rate caused no change of them due to excess supplied hydrogen. There existed a minimum gas flow rate to acquire the complete conversion of nitrobenzene. Similarly, for a given gas flow rate, increasing the liquid flow rate did not change the aniline concentration and nitrobenzene conversion due to sufficient supply of hydrogen. Once the supplied hydrogen became insufficient at high liquid flow rate, both the aniline concentration and nitrobenzene conversion were decreased. Based on these results, the excess ratios were achieved under different conditions. It was found that the excess ratio decreased with the increase of the liquid flow rate and inlet nitrobenzene concentration as a result of the enhanced mass transport. The obtained results in this work are beneficial for optimizing the gas-liquid-solid microreactor operation.

1. Introduction

Aniline is an important organic chemical material and fine chemical intermediates, which has been extensively used in synthesizing the accelerator, antioxidant, stabilizer, antidetonant, etc [1]. Until now, various methods such as the iron reduction of nitrobenzene, amination of phenol, direct amination of benzene and hydrogenation of nitrobenzene have been reported for aniline preparation [2–5]. Among these methods, the gas-liquid-solid reactor for hydrogenation of nitrobenzene has been widely used in industrial production because of its high conversion rate and selectivity of aniline as well as mild reaction conditions. In the gas-liquid-solid reactor system, gas reactants usually need to transport through the gas-liquid interfaces and liquid film to the solid catalysts, leading to a quite large mass transfer resistance. Therefore, in order to overcome the mass transfer limitation, high pressure is generally required to increase the amount of dissolved

* Corresponding author at: Institute of Engineering Thermophysics, Chongqing University, Chongqing 400030, China.
E-mail address: zhuxun@cqu.edu.cn (X. Zhu).

http://dx.doi.org/10.1016/j.cej.2016.08.011
1385-8947/

gases [6], which may potentially increase the explosion risk, specially when the activities of catalysts are high. Microreactors with the intrinsic large surface-area-to-volume ratio have been proven to be able to dramatically facilitate the mass transport of both reactants and products, allowing gas reactants to be efficiently transferred to the catalyst surface [7–11]. In addition, profited from the small volume and reaction time, the potential risk can be reduced as compared to those conventional reactors. Because of these merits, the gas-liquid-solid microreactors have been widely studied for hydrogenation of nitrobenzene.

At present, metallic nanoparticles including copper [12], nickel [13], platinum [8,14], palladium [15–17] have been extensively employed for hydrogenation of nitrobenzene, which are usually immobilized in microreactors by a variety of attempts. For example, Pd catalysts wrapped in polymers were chemically bonded to the inner surface of a glass-made microreactor [7]. Pt nanoparticle suspension was adsorbed on the wall of a microchannel coated with the supporting materials, such as titania, silica, carbon nanotube, etc [8]. Pd layer was coated on the plate by using sputtering process [18] or Pd precursor solutions were impregnated on the alumina, zeolites, etc, and then reduced [19–21]. Although the catalyst layer prepared by these methods can provide good catalytic activity, the calcination is typically required to improve the binding between the catalysts, supporting materials and substrate, which not only makes it difficult to select proper materials and prepare the microreactors but also increases the manufacturing costs. Therefore, a catalyst layer that can show high activity with easy immobilization is needed for hydrogenation of nitrobenzene.

On the other hand, previous works [22–24] have demonstrated that thin adherent polydopamine (PDA) film prepared by the self-polymerization of dopamine in aerobic condition can be formed onto a wide range of substrates with both organic and inorganic surfaces through simply immersing the substrates in a dilute aqueous solution of dopamine. Due to a large number of phenolic hydroxyl and N-containing functional groups in the surface of PDA film, an extremely versatile platform can be formed for diverse functions, such as the creation of functional organic adlayers and deposition of metallic nanoparticles by the electroless metallization on nonconductive substrates [25]. In the past, much attempt has been made to the immobilization of metal nanoparticles on the functionalized surface. For example, Ryoo et al. [26] deposited the palladium catalyst onto the polydopamine functionalized surface of the peptide nanowires for the heterogeneous catalytic reactions. Ye et al. [27] prepared Pd and Pt nanocatalysts onto the functionalized multi-walled carbon nanotubes for the electrooxidation of hydrazine and methanol, respectively. Shen et al. [28] fabricated silver coated polyacrylonitrile nanofibrous composite membrane by using this method for the degradation of methylene blue. However, due to the limited reduction ability of the polydopamine, there always existed a large amount of residual metal ions on the surface, decreasing the metal utilization. Xu and coworkers [29] introduced the extra reducing agent of glucose for the further reduction of residual silver ions in the fabrication of conductive silver layer on the glass fibers. The above literature review indicates that although the functional materials on the surface can reduce the metal ions to some extent, the reduction ability was limited. It is essential to add extra reducing agent for complete reduction of metal ions. In line with this idea, we developed a gas-liquid-solid microreactor with Pd nanoparticles deposited on the inner surface of the PDA coated microchannel by the electroless plating for hydrogenation of nitrobenzene. To decrease the residual Pd ions, the developed microreactor was further restored with the additional reducing agent of hydrogen. The chemical composition and morphology were studied by X-ray photoelectron spectroscopy (XPS) and field emission scanning electron microscopy (FESEM), respectively. The catalyst stability and activity towards nitrobenzene hydrogenation were evaluated under various operating conditions by a gas chromatograph. The relationships between the flow rate of reactants (both gaseous and liquid reactants) and the nitrobenzene conversion at various inlet nitrobenzene concentrations were also explored.

2. Experimental

2.1. Chemicals

In this work, all the chemicals were used as received. Dopamine hydrochloride was obtained from Aladdin Industrial Inc (Shanghai, China). Tris (Tris(hydroxymethyl) aminomethane) used as buffer agent was supplied by GEN-VIEW Scientific Inc (Florida, USA). Palladium chloride was purchased from Sino-platinum Metals CO. LTD (Kunming, China). Potassium chloride, ethanol, nitrobenzene were acquired from Chongqing Chuandong Chemical CO. LTD (Chongqing, China). Water used in the whole experiment was obtained from an Ultrapure Water System for Laboratory (ROMB, Chongqing, China). Commercially available PTFE (Polytetrafluoroethylene) capillary tube with the inner diameter of 0.6 mm, outer diameter of 1.0 mm and the length of 1.0 m was used as the microreactor.

2.2. Preparation and characterization of catalyst layer

As mentioned above, the polydopamine coating was formed by the self-polymerization of dopamine, which could act not only as an adhesive but also as a reducing agent [22,26]. The catalyst layer was prepared through the following stages. In the first step, a dilute aqueous dopamine solution (2 mg/mL in 10 mM Tris buffer, pH = 8.5) was fed into the PTFE capillary tube at a flow rate of 1 mL/h for 5 h, followed by flushing with water at a flow rate of 0.5 mL/min for 20 min, and then heated at 338 K for 1 h under nitrogen atmosphere. By do this, a polydopamine layer in the inner wall of the PTFE capillary tube could be obtained. In the second step, to deposit Pd nanoparticles on the PDA layer, 5 mM K_2PdCl_4 aqueous solution was firstly prepared by dissolving $PdCl_2$ and KCl in water ($PdCl_2$: 886.65 μg/mL and KCl: 372.75 μg/mL) and then infiltrated into the PTFE capillary tube with coated PDA film at a flow rate of 0.1 μL/min for 12 h for the adsorption and reduction of Pd ions. After that, to remove the residual ions, the PTFE capillary tube was flushed with excess amount of water several times at a flow rate of 10 μL/min. Finally, to further reduce the residual palladium ions and increase the utilization of palladium ions, the PTFE capillary tube coated with a Pd-PDA layer was placed into the vacuum tube resistance furnace (Tianjin Zhonghuan Lab Furnace Co., Ltd, China) and then heated in the H_2 environment under 473 K for 4 h. The surface chemical compositions of the sample surfaces were characterized by using XPS system (ESCALAB 250Xi, Thermo, USA) with Al Kα radiation (hν = 1486.6 eV) at a power of 150 W. The surface topography of the samples was acquired by using FESEM (S4800, Hitachi High Technologies, Japan) fulfilled at an accelerating voltage of 3 kV. Prior to the test, the surfaces of the samples were sputtered with platinum.

2.3. Experimental setup

Fig. 1 shows the schematic diagram of the microreactor and the experimental system. Taking into consideration that a spiral channel pattern can not only enhance the heat and mass transfer and reduce pressure drop but also decrease the space requirement, the PTFE capillary tube coated with a Pd-PDA catalyst layer was wrapped around a stainless steel tube with the external diameter of 0.5 in. to form the microreactor (see Fig. 1a). Meanwhile, to simultaneously supply the gaseous and liquid reactants stably, a

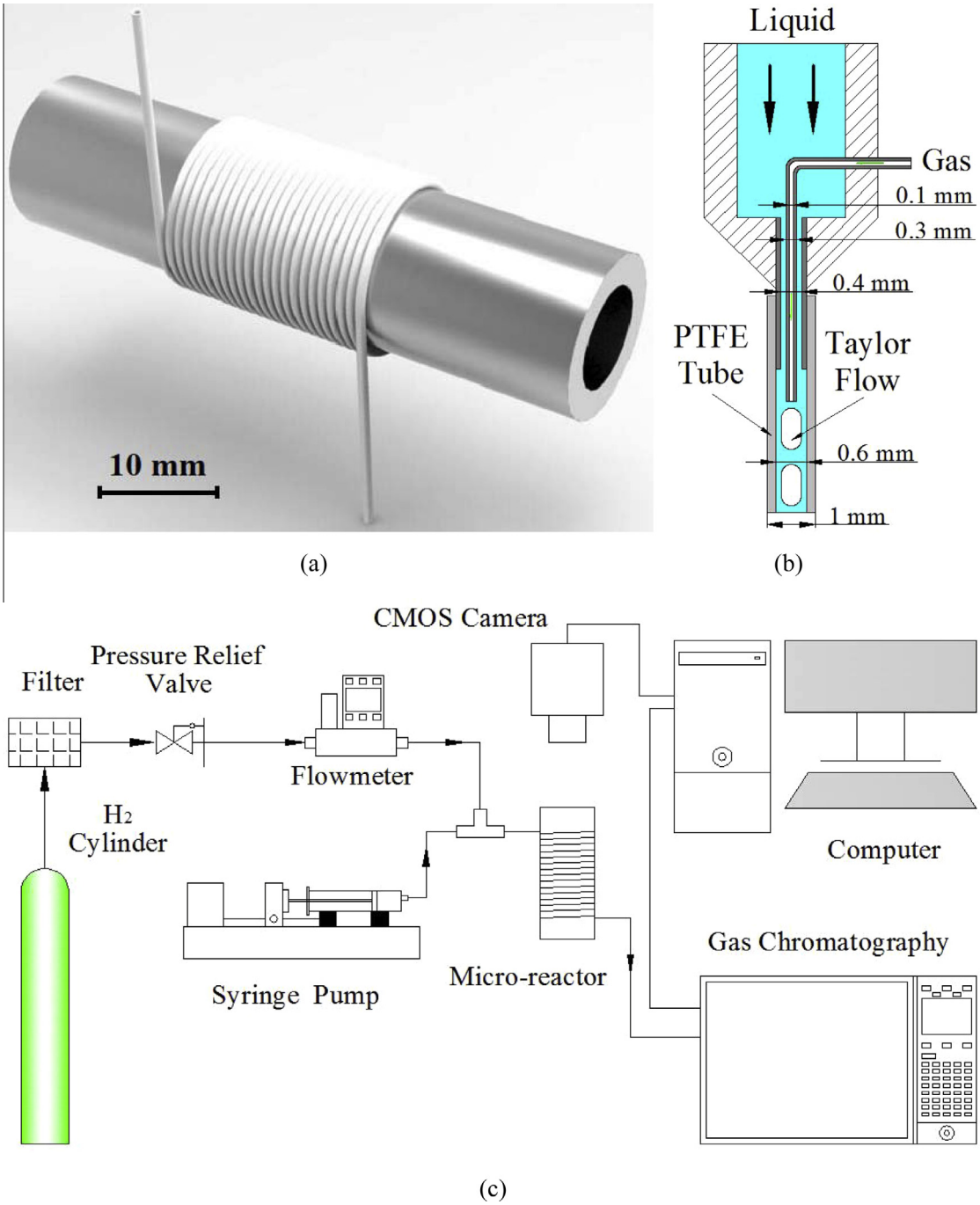

Fig. 1. Schematic of (a) the microreactor, (b) the connector and (c) the experimental system.

home-made connector was adopted in this experiment, as shown in Fig. 1b. During the operation, the liquid reactant prepared by dissolving nitrobenzene (Analytical Reagent) in ethanol with the ethanol: water = 7:3 in volume and high-purity hydrogen were simultaneously fed into the microreactor using a syringe pump (LSP01-1BH, Longer-Pump, China) and a mass flow controller (FMA-2602A-I, Omega, USA), respectively (see Fig. 1c). A gas-liquid Taylor flow was then formed inside the microreactor. Since the PTFE capillary tube had the inner diameter of 0.6 mm and the outer diameter of 1.0 mm, the corresponding wall thickness was about 200 μm. Such a thin thickness made the PTFE capillary tube semi-transparent, which allows us to capture the images of the flow pattern inside the microreactor by a CMOS camera (GS3-U3-41C6M-C, PointGray, Canada). The effluent was collected to measure the concentrations of nitrobenzene and the desired product of aniline by a gas chromatograph (GC-2010 Plus, Shimadzu, Japan) equipped with a flame ionization detector (FID). Separation of the reaction products was performed by means of a capillary column (Rtx-1301, 30 m × 0.32 mm, Restek, USA). Nitrogen gas (High Purity) was used as the mobile phase.

3. Results and discussions

3.1. Materials characterizations

To elaborate the formation of the Pd-PDA layer in the microreactor, the chemical compositions of the original and PDA modified

PTFE and the Pd coated PDA layer were characterized by XPS. The results are presented in Fig. 2. As shown in Fig. 2a, for the PTFE surface before the modification with dopamine, three peaks appeared at 292.25 eV (C 1s), 532.07 eV (O 1s) and 689.35 eV (F 1s), indicating that the PTFE material mainly contained carbon and fluorine and a small amount of oxygen (content = 0.91 mol%). The existence of oxygen may be caused by the adsorption of oxygen from the air [30]. Fig. 2b shows the XPS spectra of the PTFE sample modified with dopamine, in which four peaks could be clearly seen at 284.8 eV (C 1s), 400.49 eV (N 1s), 532.15 eV (O 1s) and 689.38 eV (F 1s). Compared with the result shown in Fig. 2a, one extra peak at 399.82 eV (N 1s) could be observed obviously in the XPS spectrum of the modified PTFE. The existence of nitrogen suggested that a PDA layer had been successfully adhered to the inner surface of the PTFE capillary tube through the self-polymerization of dopamine. Fig. 2c shows the XPS spectra of Pd coated PDA layer. It can be seen that the difference between Pd coated and uncoated PDA layers lied in that there existed two additional peaks at 335.52 eV and 340.77 eV, which were assigned to Pd^0 ($3d_{5/2}$) and Pd^0 ($3d_{3/2}$), respectively. This result demonstrates the metallic Pd has been successfully prepared and immobilized on the PDA layer.

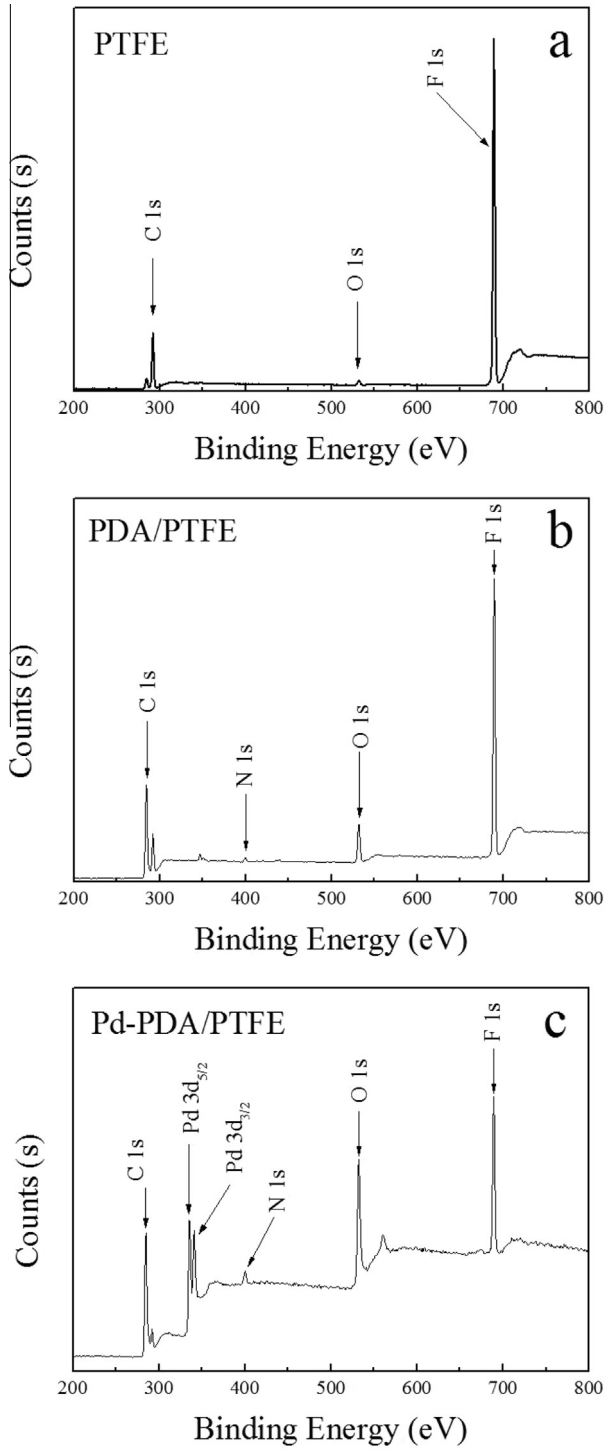

Fig. 2. XPS spectra of (a) PTFE, (b) PDA/PTFE and (c) Pd-PDA/PTFE.

Fig. 3 shows the FESEM images of the pristine PTFE, PDA/PTFE and Pd-PDA/PTFE. By comparing the FESEM images of the pristine PTFE and PDA/PTFE, it can be seen that a uniform PDA layer has been formed on the PTFE surface. In addition, as shown in Fig. 3c, after the deposition of Pd, Pd nanoparticles with the mean particle size of about 50 nm were observed on the PDA surface. Moreover, Pd nanoparticles were uniformly distributed over the surface of PDA layer. Based on the FESEM results, the particle size distribution was also obtained. As shown in Fig. 4a, the sizes of the discrete Pd nanoparticles were uniform and more than half of the nanoparticles lied in the range of about 50 nm. The thickness of the catalyst layer was also characterized in this work. Fig. 4b shows the cross-sectional image of the Pd-PDA layer coated inner surface of the PTFE capillary tube. The observation suggested that the thickness of the Pd-PDA layer was only about 70–80 nm. Such a thin layer is enough for the light transmission, allowing us to visualize the two-phase flow patterns in the microreactor.

3.2. Performance evaluation

To evaluate the performance of the developed microreactor, the long-term operation for 40 h was carried out. In this measurement, the gas flow rate was kept at 0.05 sccm and the liquid flow rate was maintained at 5 μL/min. The inlet nitrobenzene ranged from 30 mM to 90 mM. The effluents from the outlet were collected every two hour. Fig. 5a shows the variation of the nitrobenzene conversion under different inlet nitrobenzene concentrations. As shown, over the entire operation period, the average aniline concentrations at the outlet were 29.36 mM, 58.31 mM and 87.93 mM with respect to the inlet nitrobenzene concentration of 30 mM, 60 mM and 90 mM, respectively. The corresponding average nitrobenzene conversions were 97.4%, 97.2% and 97.5%, as shown in Fig. 5b. Such high nitrobenzene conversions under different inlet nitrobenzene concentrations can be attributed to enhanced mass transfer in the microreactor and excellent catalytic activity of the prepared catalyst layer, both of which facilitated hydrogenation of nitrobenzene to yield good performance. Moreover, it can be seen that the nitrobenzene conversion was rather stable, as shown in Fig. 5a. It is indicated that the catalysts have been strongly adhered to the PDA layer to enhance the operation stability. On the other hand, because of enhanced mass transport, the products including the intermediates can be efficiently removed, avoiding the catalyst poison and thereby further improving the stability. In summary, the microreactor with the coated Pd-PDA layer can yield good and stable performance.

3.3. Effect of the flow rate

In this experiment, hydrogen and nitrobenzene were simultaneously fed into the microreactor, forming a typical gas-liquid Taylor flow. Both the gas and liquid flow rates will play a significant role in influencing the flow pattern and thereby the performance of the microreactor. For this reason, the effects of both the gas and liquid flow rates were investigated and the results are discussed in the following.

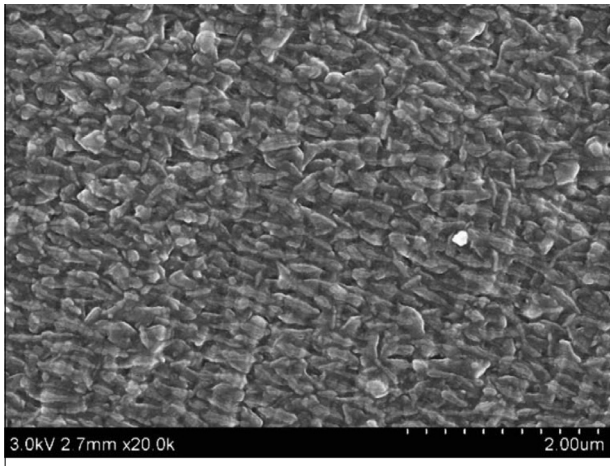

(a)

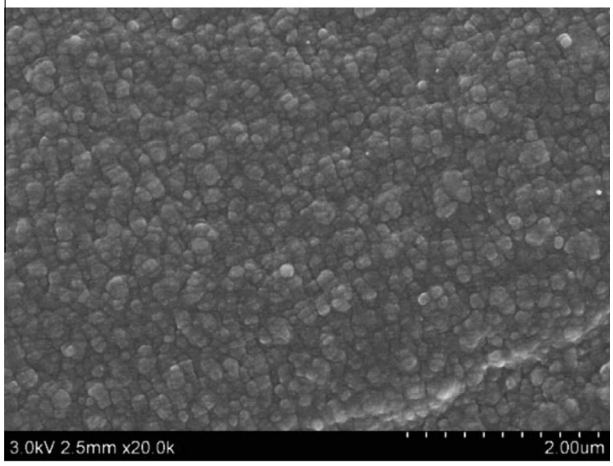

(b)

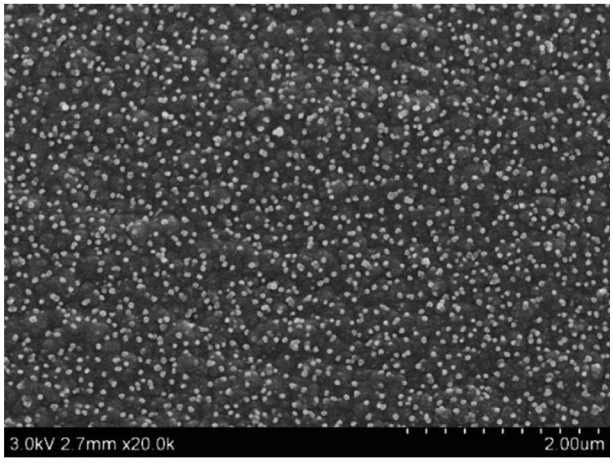

(c)

Fig. 3. FESEM images of (a) PTFE, (b) PDA/PTFE and (c) Pd-PDA/PTFE surface.

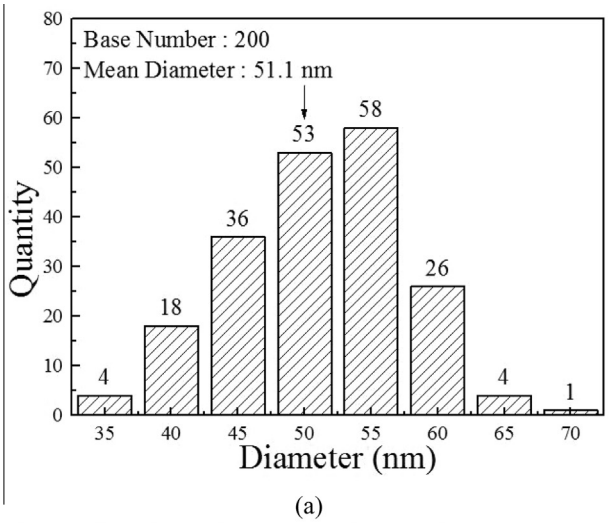

(a)

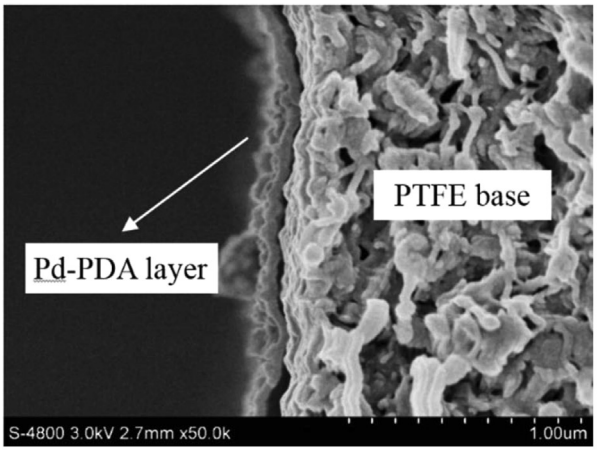

(b)

Fig. 4. (a) Size distribution of Pd nanoparticles on the PDA layer and (b) FESEM images of the cross section of the Pd-PDA/PTFE.

3.3.1. Gas flow rate

In this section, the liquid flow rate was kept at 20 μL/min, while the feeding nitrobenzene concentrations were 30 mM, 60 mM and 90 mM, respectively. As shown in Fig. 6, with the increment of the gas flow rate, the aniline concentration of the effluent was firstly increased and then reached a stable value. It is easy to understand that at low gas flow rates, the supply of gas reactant was insufficient so that only a part of nitrobenzene could participate the catalytic reaction. An increase in the gas flow rate led to more gas reactant supplied to the microreactor for the catalytic reaction. As a result, more aniline could be produced, resulting in the increase of the aniline concentration. Meanwhile, higher aniline concentration would be achieved with increasing the inlet nitrobenzene concentration under the same gas and liquid flow rates. This is because more nitrobenzene was supplied and larger nitrobenzene concentration created a larger concentration gradient from the bulk to the active surface, enhancing the mass transport and thereby producing more aniline. As the gas flow rate was further increased, excess hydrogen was fed into the microreactor to ensure the all supplied nitrobenzene to be involved into the catalytic reaction. In this case, the aniline concentration approached to the inlet nitrobenzene concentration. Further increasing the gas flow rate would not change the aniline concentration due to the limited supply of nitrobenzene. Corresponding to the variations of the aniline concentration, the nitrobenzene conversion was also firstly increased at low gas flow rate and then maintained at 97%, (see Fig. 6b).

From the above results, it can be found that for a given liquid flow rate, with the increase of the gas flow rate, the catalytic reaction experienced two stages: insufficient and excess supply of hydrogen. The change point represented the minimum hydrogen consumption rate, assuming the complete utilization of hydrogen with a 100% conversion of nitrobenzene. Because the complete conversion of one mole nitrobenzene produces one mole aniline

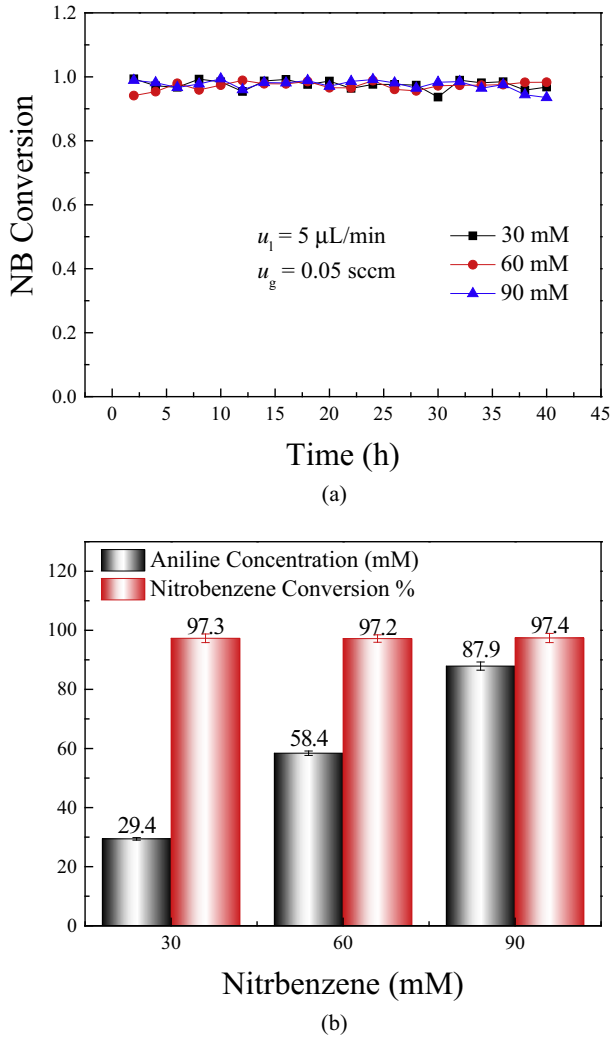

Fig. 5. (a) Variations of the nitrobenzene conversion with the operation time under different inlet nitrobenzene concentrations, and (b) change of the average aniline concentration and nitrobenzene conversion.

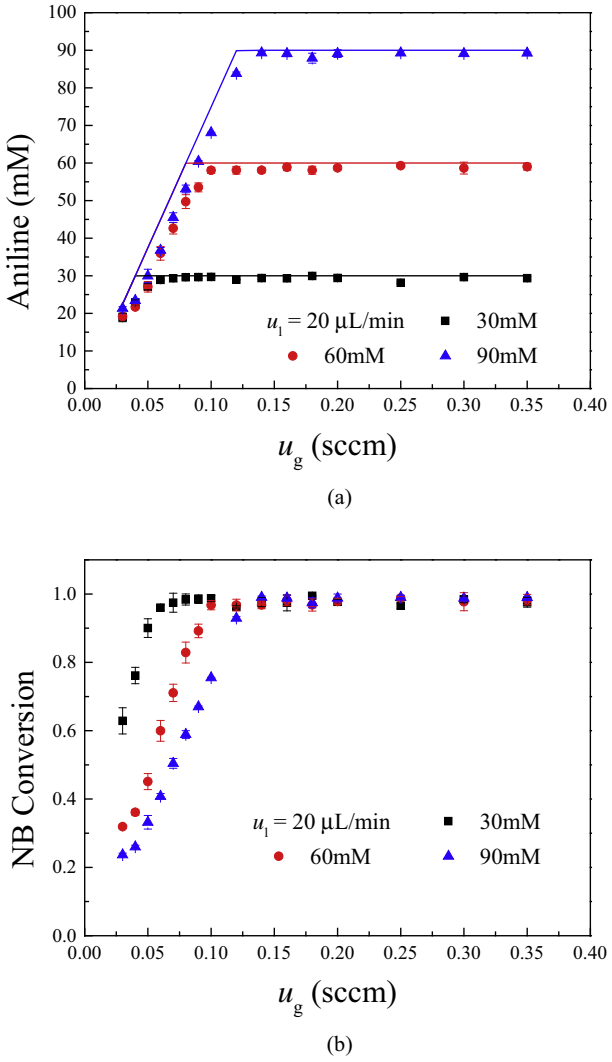

Fig. 6. Effect of the gas flow rate on (a) the aniline concentration and (b) the NB conversion.

($C_6H_5NO_2 + 3H_2 \rightarrow C_6H_5NH_2 + 2H_2O$), the aniline concentration of each stage at the outlet could be written as follows,

$$C_{an} = \frac{u_g}{u_{g,min}} \cdot C^0_{nb} \quad (u_g < u_{g,min}) \tag{1}$$

$$C_{an} = C^0_{nb} \quad (u_g \geqslant u_{g,min}) \tag{2}$$

where C_{an} represents the aniline concentration in the effluent, C^0_{nb} is the inlet nitrobenzene concentration, u_g stands for the gas flow rate and $u_{g,min}$ is the minimum gas flow rate corresponding to the 100% nitrobenzene conversion. With the above equations, the minimum gas flow rate could be calculated by

$$u_{g,min} = \frac{\eta \cdot C^0_{nb} \cdot M_g \cdot u_l}{\rho_{g,STP}} \tag{3}$$

where u_l represents the liquid flow rate, M_g = 2 g/mol and $\rho_{g,STP}$ = 0.0899 g/L are the molar mass and density of hydrogen at the standard temperature and pressure of 273.15 K and 101.325 kPa, η = 3 is the stoichiometric ratio of hydrogen to nitrobenzene. Thus, the relationship between C_{an} and u_g can be obtained,

$$C_{an} = \frac{\rho_{g,STP} \cdot u_g}{\eta \cdot M_g \cdot u_l} \quad (u_g < u_{g,min}) \tag{4}$$

$$C_{an} = C^0_{nb} \quad (u_g \geqslant u_{g,min}) \tag{5}$$

The results calculated by these two equations are shown in Fig. 6a, indicated by the solid line. The minimum gas flow rates from low nitrobenzene concentration to high concentration were 40.0×10^{-3} sccm (30 mM), 80.1×10^{-3} sccm (60 mM) and 120.1×10^{-3} sccm (90 mM), respectively. The experimental results are well in agreement with the calculated results. However, the minimum gas flow rates measured by experiments were slightly larger than those calculated values and the aniline concentrations at the gas flow rates below the change point were also slightly smaller. This is because the calculated results are based on the assumption of the complete conversion with eliminating the effect of the mass transport. In reality, during the gas-liquid-solid reaction process, the volumetric fraction of hydrogen gradually decreased, indicating that the length of liquid slug increased and gas slug decreased, as evidenced by the captured images in Fig. 7. In this case, the hydrogen concentration over the entire microreactor became rather non-uniform and the resistance of mass transfer would be intensified, slowing down the reaction rate. Therefore, the produced aniline was lower than the predicted values at low gas flow rates. Meanwhile, there existed a concentration gradient to ensure the transfer of hydrogen to the catalyst layer. Under such a circumstance, more hydrogen was needed to ensure

the complete conversion of nitrobenzene so that the measured minimum gas flow rate was slightly higher than the predicted value. However, once the supplied became excess, the above problems were weakened. This fact indicates that to guarantee the complete conversion of nitrobenzene to aniline, a slightly higher gas flow rate is required in real operations.

3.3.2. Liquid flow rate

In this experiment, three inlet nitrobenzene concentrations of 30 mM, 60 mM and 90 mM were selected. The gas flow rate was kept at 0.05 sccm, while the liquid flow rate ranged from 5 μL/min to 25 μL/min. Fig. 8 shows the variations of the aniline concentration and nitrobenzene conversion with the liquid flow rate under different inlet concentrations. Obviously, for a given gas flow rate, the aniline concentration (see Fig. 8a) and nitrobenzene conversion (see Fig. 8b) was firstly kept unchanged and then decreased at low nitrobenzene concentration of 30 mM. They were always quickly decreased with increasing the liquid flow rate at high nitrobenzene concentration of 90 mM, while both of them slightly decreased with increasing the liquid flow rate from 5 μL/min and then quickly decreased as the liquid flow rate was further increased at the moderate nitrobenzene concentration of 60 mM. The reasons leading to these phenomena are described as follows. For a given gas flow rate, the supplied nitrobenzene at low liquid flow rates could be fully utilized to generate aniline at low inlet nitrobenzene concentration of 30 mM. As a result, the aniline concentrations were quite close to the inlet nitrobenzene concentrations and the corresponding nitrobenzene conversions were nearly 100%. As the liquid flow rate increased, the supplied hydrogen might be insufficient, leading to the decrease of the aniline concentration and nitrobenzene conversion. For the moderate inlet nitrobenzene concentration of 60 mM, at low liquid flow rate of 5 μL/min, the supplied hydrogen could meet the complete reaction requirement so that the aniline concentration was close to the inlet nitrobenzene and the nitrobenzene conversion approached to 100%. As the liquid flow rate increased to 10 μL/min, the supplied hydrogen started to become insufficient but could still meet the most requirement for hydrogenation of nitrobenzene. Hence, the aniline concentration and nitrobenzene conversion were slightly decreased. However, as the liquid flow rate was further increased, the supplied hydrogen became greatly insufficient such that the aniline concentration and nitrobenzene conversion were quickly decreased. As for high inlet nitrobenzene concentration of 90 mM, the supplied liquid reactant was greatly increased. Hence, except the nitrobenzene conversion could reach about 100%, the increase of the liquid flow rate also caused a quick reduction in the aniline concentration and nitrobenzene conversion. Similarly, for a given gas flow rate, the relationship between C_{an} and u_l can be written as,

$$C_{an} = \frac{u_{l,max}}{u_l} \cdot C_{nb}^0 \quad (u_l > u_{l,max}) \tag{6}$$

$$C_{an} = C_{nb}^0 \quad (u_l \leqslant u_{l,max}) \tag{7}$$

where $u_{l,max}$ is the maximum liquid flow rate corresponding to 100% nitrobenzene conversion, which could be determined by

$$u_{l,max} = \frac{\rho_{g,STP} \cdot u_g}{\eta \cdot C_{nb}^0 \cdot M_g} \tag{8}$$

Based on Eqs. (6)–(8), the relationship between C_{an} and u_l could be rewritten as,

$$C_{an} = \frac{\rho_{g,STP} \cdot u_g}{\eta \cdot M_g \cdot u_l} \quad (u_l > u_{l,max}) \tag{9}$$

$$C_{an} = C_{nb}^0 \quad (u_l \leqslant u_{l,max}) \tag{10}$$

The results calculated by these two equations are indicated by the solid line in Fig. 8a. As seen, compared with the experimental results, the maximum liquid flow rate measured from the experiment was smaller than these calculated values. This may be due to the mass transport resistance of hydrogen between the phases, which led to early occurrence of the reaction equilibrium and thereby smaller maximum liquid flow rate measured by the experiment.

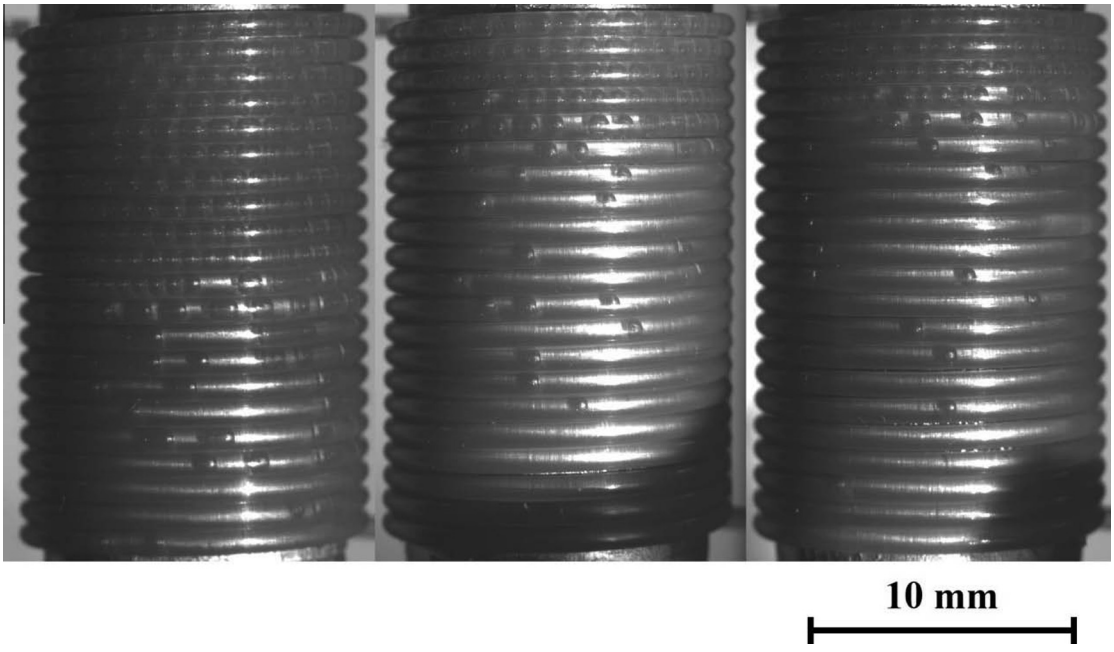

Fig. 7. Image of the slug flow characteristics in the microreactor at u_g = 0.05 sccm, u_l = 20 μL/min and the inlet nitrobenzene concentration ranging from 30 mM to 90 mM.

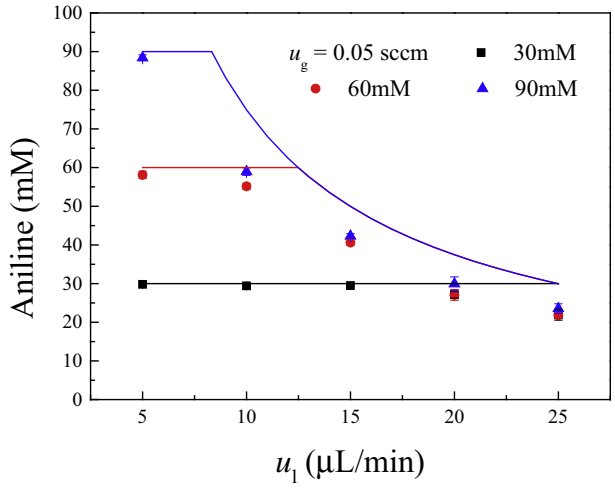

(a)

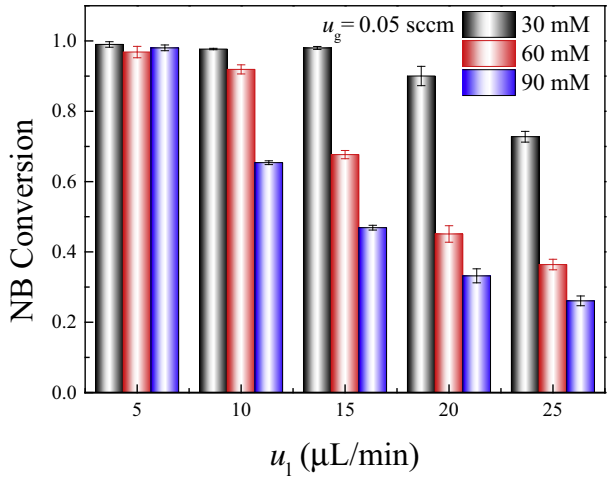

(b)

Fig. 8. Effect of the liquid flow rate on (a) the aniline concentration and (b) the NB conversion.

3.4. Excess ratio

From the above analysis on the effect of both the gas and liquid flow rates, it could be found that, to reach a critically high nitrobenzene conversion, excess gaseous reactant should be fed into the reactor. For a given nitrobenzene concentration, there exists a ratio of a minimum gas flow rate to theoretical value for enabling the complete nitrobenzene conversion. Therefore, in this study, the nitrobenzene conversions at various conditions (gas flow rate ranging from 0.01 sccm to 0.35 sccm, liquid flow rate ranging from 5 μL/min to 25 μL/min and inlet concentration ranging from 30 mM to 90 mM) were summarized. These conditions corresponded to high conversion rate (⩾97%) with the smallest required gas flow rate. The minimum gas flow rates for the complete nitrobenzene conversion under different inlet nitrobenzene concentrations and liquid flow rates along with the solid lines fitted by these data are shown in Fig. 9a. The theoretical values under these conditions are also shown in Fig. 9a, as indicated by the dash lines. It can be seen that increasing the liquid flow rate and inlet nitrobenzene concentration led to an improvement in the minimum gas flow rate for the complete nitrobenzene conversion as a result of the increase of the supplied nitrobenzene. Based on these results, the excess ratio could then be calculated and the results are shown in Fig. 9b. As seen, the excess ratio was gradually decreased with the increase of the liquid flow rate. It is easy to understand that increasing the liquid flow rate resulted in the increase of the supplied nitrobenzene so that more gaseous reactant supply of hydrogen is needed. The increased gas flow rate would enhance the mass transport between the phases for both reactants and products, enhancing the utilization of gaseous reactant and thereby decreasing the excess ratio. In addition, the excess ratio in the case of low inlet nitrobenzene concentration was larger than that at high concentration. This may be attributed to two reasons. On one hand, high inlet nitrobenzene concentration required more gaseous reactant, which accordingly increased the gas flow rate, leading to the enhancement of the mass transfer of hydrogen. On the other hand, high inlet nitrobenzene concentration was beneficial for the reaction and formed a relatively high nitrobenzene concentration gradient as compared with low inlet nitrobenzene concentration, which would intensify the mass transport of nitrobenzene. Therefore, the gaseous reactant utilization efficiency under high inlet nitrobenzene concentration was enhanced so that the excess ratio decreased as the inlet nitrobenzene concentration

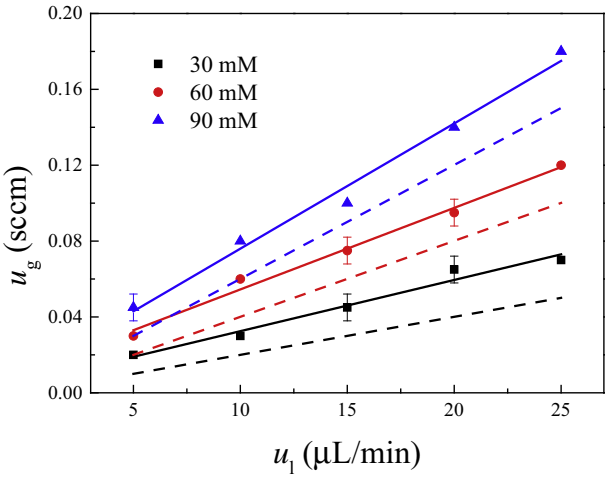

(a)

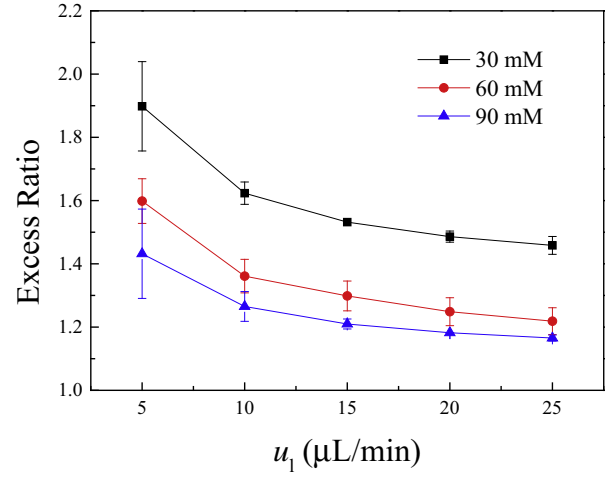

(b)

Fig. 9. (a) Influence of the liquid flow rate and inlet nitrobenzene concentration on the minimum gas flow rate for the complete nitrobenzene conversion (Point: experimental data, Solid line: fitted curve from experimental data, Dash line: theoretical value calculated from Eq. (3)). (b) Influence of the liquid flow rate and inlet nitrobenzene concentration on the excess ratio.

increased. The above results are useful for designing the real operation conditions.

4. Conclusions

In this study, a gas-liquid-solid microreactor with the polydopamine functionalized surface for coating palladium nanoparticles by the electroless deposition was developed for hydrogenation of nitrobenzene. Both the surface chemical composition and topography characterizations indicated that the inner surface of the microreactor was successfully modified with the polydopamine and Pd nanoparticles were well deposited on the modified surface. The long-term performance of the developed microreactor was evaluated. It was shown that not only high nitrobenzene conversion but also good stability were achieved in a range of the inlet nitrobenzene concentration from 30 mM to 90 mM. The effects of the gas flow rate and liquid flow rate were also visited. The results showed that for a given liquid flow rate and inlet nitrobenzene concentration, increasing the gas flow rate firstly led to an increase in the aniline concentration and nitrobenzene conversion. Once the supplied hydrogen can meet the complete conversion of nitrobenzene, the aniline concentration became stable and the nitrobenzene conversion was almost 100%. Similarly, for a given gas flow rate and inlet nitrobenzene concentration, when the supplied hydrogen enabled the complete conversion of nitrobenzene, increasing the liquid flow rate showed no effect on the aniline concentration and the nitrobenzene conversion. However, once the supplied hydrogen cannot meet this requirement, both the aniline concentration and nitrobenzene conversion decreased with increasing the liquid flow rate. It was also found that because of the mass transport resistance of hydrogen between phases, excess hydrogen needed to be supplied as compared to the theoretical values. Excess ratio was thus defined to show this effect. The experimental results revealed that increasing the inlet nitrobenzene concentration and the liquid flow rate could lead to a reduction in the excess ratio as a consequence of enhanced mass transfer.

Acknowledgments

The authors gratefully acknowledge the financial supports of the National Natural Science Foundation of China (No. 51276208, No. 51325602, No. 51222603), Specialized Research Fund for the Doctoral Program of Higher Education of China (No. 20120191110010), Program for New Century Excellent Talents in University (NCET-12-0591) and Chongqing Graduate Student Research Innovation Project (No. CYB14012).

References

[1] T. Sheng, Y.J. Qi, X. Lin, P. Hu, S.G. Sun, W.F. Lin, Insights into the mechanism of nitrobenzene reduction to aniline over Pt catalyst and the significance of the adsorption of phenyl group on kinetics, Chem. Eng. J. 293 (2016) 337–344.
[2] P. Desrosiers, S.H. Guan, A. Hagemeyer, D.M. Lowe, C. Lugmair, D.M. Poojary, H. Turner, H. Weinberg, X.P. Zhou, R. Armbrust, G. Fengler, U. Notheis, Application of combinatorial catalysis for the direct amination of benzene to aniline, Appl. Catal. A Gen. 227 (2002) 43–61.
[3] T. Yu, Q. Zhang, S. Xia, G. Li, C. Hu, Direct amination of benzene to aniline by reactive distillation method over copper doped hierarchical TS-1 catalyst, Catal. Sci. Technol. 4 (2014) 639–647.
[4] C.H. Li, Z.X. Yu, K.F. Yao, S.F. Ji, J. Liang, Nitrobenzene hydrogenation with carbon nanotube-supported platinum catalyst under mild conditions, J. Mol. Catal. A Chem. 226 (2005) 101–105.
[5] G.Y. Fan, W.J. Huang, Solvent-free hydrogenation of nitrobenzene catalyzed by magnetically recoverable Pt deposited on multi-walled carbon nanotubes, Synth. React. Inorg. Met.-Org. Nano-Met. Chem. 45 (2015) 1819–1825.
[6] G.A. Somorjai, F. Heinz, J.Y. Park, Advancing the frontiers in nanocatalysis, biointerfaces, and renewable energy conversion by innovations of surface techniques, J. Am. Chem. Soc. 131 (2009) 16589–16605.
[7] J. Kabayashi, Y. Mori, K. Okamoto, R. Akiyama, M. Ueno, T. Kitamori, S. Kobayashi, A microfluidic device for conducting gas-liquid-solid hydrogenation reactions, Science 304 (2004) 1305–1308.
[8] S. Kataoka, Y. Takeuchi, A. Harada, T. Takagi, Y. Takenaka, N. Fukaya, H. Yasuda, T. Ohmori, A. Endo, Microreactor containing platinum nanoparticles for nitrobenzene hydrogenation, Appl. Catal. A Gen. 427–428 (2012) 119–124.
[9] S. Kataoka, A. Endo, M. Oyama, T. Ohmori, Enzymatic reactions inside a microreactor with a mesoporous silica catalyst support layer, Appl. Catal. A Gen. 359 (2009) 108–112.
[10] L.N. Protasova, E.V. Rebrov, T.S. Glazneva, A. Berenguer-Murcia, Z.R. Ismagilov, J.C. Schouten, Control of the thickness of mesoporous titania films for application in multiphase catalytic microreactors, J. Catal. 271 (2010) 161–169.
[11] N. Kockmann, M. Gottsponer, D.M. Roberge, Scale-up concept of single-channel microreactors from process development to industrial production, Chem. Eng. J. 167 (2011) 718–726.
[12] S. Diao, W. Qian, G. Luo, F. Wei, Y. Wang, Gaseous catalytic hydrogenation of nitrobenzene to aniline in a two-stage fluidized bed reactor, Appl. Catal. A Gen. 286 (2015) 30–35.
[13] F. Alonso, P. Riente, J.A. Sirvent, M. Yus, Nickel nanoparticles in hydrogen-transfer reductions: characterisation and nature of the catalyst, Appl. Catal. A Gen. 378 (2010) 42–51.
[14] Y. Zhao, C.H. Li, Z.X. Yu, K.F. Yao, S.F. Ji, J. Liang, Effect of microstructures of Pt catalysts supported on carbon nanotubes (CNTs) and activated carbon (AC) for nitrobenzene hydrogenation, Mater. Chem. Phys. 103 (2007) 225–229.
[15] L. Pikna, M. Heželová, S. Demčáková, M. Smrčová, B. Plešingerová, M. Štefanko, M. Turáková, M. Králik, P. Puliš, Effect of support on activity of palladium catalysts in nitrobenzene hydrogenation, Chem. Pap. 68 (2014) 591–598.
[16] M. Turáková, M. Králik, P. Lehocký, Ľ. Pikna, M. Smrčová, D. Remeteiová, A. Hudák, Influence of preparation method and palladium content on Pd/C catalysts activity in the liquid phase hydrogenation of nitrobenzene to aniline, Appl. Catal. A Gen. 476 (2014) 103–112.
[17] R. Yan, J.X. Xu, Y. Zhang, D. Wang, M.C. Zhang, W.Q. Zhang, Simultaneous Pd catalyst immobilization during synthesis of mesoporous silica, Chem. Eng. J. 200–202 (2012) 559–568.
[18] K.K. Yeong, A. Gavriilidis, R. Zapf, V. Hessel, Catalyst preparation and deactivation issues for nitrobenzene hydrogenation in a microstructured falling film reactor, Catal. Today 81 (2003) 641–651.
[19] G. Guan, K. Kusakabe, M. Taneda, M. Uehara, H. Maeda, Catalytic combustion of methane over Pd-based catalyst supported on a macroporous alumina layer in a microchannel reactor, Chem. Eng. J. 144 (2008) 270–276.
[20] J.L. Chau, A.Y. Leung, K.L. Yeung, Zeolite micromembranes, Lab Chip 3 (2003) 53–55.
[21] T. Zhang, X.F. Zhang, X.J. Yan, L. Lin, H.O. Liu, J.S. Qiu, K.L. Yeung, Core–shell Pd/ZSM-5@ZIF-8 membrane micro-reactors with size selectivity properties for alkene hydrogenation, Catal. Today 236 (2014) 41–48.
[22] H. Lee, S.M. Dellatore, W.M. Miller, P.B. Messersmith, Mussel-inspired surface chemistry for multifunctional coatings, Science 318 (2007) 426–430.
[23] B. Li, W.P. Liu, Z.Y. Jiang, X. Dong, B. Wang, Y. Zhong, Ultrathin and stable active layer of dense composite membrane enabled by poly(dopamine), Langmuir 25 (2009) 7368–7374.
[24] B.P. Lee, P.B. Messersmith, J.N. Israelachvili, J.H. Waite, Mussel-inspired adhesives and coatings, Annu. Rev. Mater. Res. 41 (2011) 99–132.
[25] S. Shi, L.B. Wang, R.X. Su, B.S. Liu, R.L. Huang, W. Qi, Z.M. He, A polydopamine-modified optical fiber SPR biosensor using electroless-plated gold films for immunoassays, Biosens. Bioelectron. 74 (2015) 454–460.
[26] H.I. Ryoo, J.S. Lee, C.B. Park, D.P. Kim, A microfluidic system incorporated with peptide/Pd nanowires for heterogeneous catalytic reactions, Lab Chip 11 (2011) 378–380.
[27] W. Ye, H. Hu, H. Zhang, F. Zhou, W. Liu, Multi-walled carbon nanotube supported Pd and Pt nanoparticles with high solution affinity for effective electrocatalysis, Appl. Surf. Sci. 256 (2010) 6723–6728.
[28] L.D. Shen, L.N. Yu, M. Wang, X.F. Wang, M.F. Zhu, B.S. Hsiao, Green fabrication of Ag coated polyacrylonitrile nanofibrous composite membrane with high catalytic efficiency, J. Nanosci. Nanotechnol. 15 (2015) 5004–5012.
[29] C.H. Xu, M. Tian, L. Liu, H. Zou, L.Q. Zhang, W.C. Wang, Fabrication and properties of silverized glass fiber by dopamine functionalization and electroless plating, J. Electrochem. Soc. 159 (2012). D217–D224.
[30] Z.Y. Xi, Y.Y. Xu, L.P. Zhu, Y. Wang, B.K. Zhu, A facile method of surface modification for hydrophobic polymer membranes based on the adhesive behavior of poly(DOPA) and poly(dopamine), J. Membr. Sci. 327 (2009) 244–253.